Forest Ecology and Management 517 (2022) 120268

Contents lists available at ScienceDirect

Forest Ecology and Management

journal homepage: www.elsevier.com/locate/foreco

Growth history of pollarded black poplars in a continental Mediterranean region: A paradigm of vanishing landscapes

J. Julio Camarero [a,*], Ester González de Andrés [a], Michele Colangelo [a,b], Chabier de Jaime Loren [c]

[a] Instituto Pirenaico de Ecología (CSIC), Apdo. 202, 50192 Zaragoza, Spain
[b] School of Agricultural, Forest, Food and Environmental Sciences (SAFE), University of Basilicata, 85100 Potenza, Italy
[c] Parque Cultural del Chopo Cabecero del Alto Alfambra, 44159 Aguilar del Alfambra, Spain

ARTICLE INFO

Keywords:
Dendroecology
Floodplain forest
Land-use changes
Pollarded trees
Populus nigra
River flow
Teruel

ABSTRACT

Pollarded woodlands are iconic components of European rural landscapes. Pollarding is a traditional management technique used to obtain timber and firewood. However, these woodlands are subjected to different stressors in rapidly depopulating rural regions under continental Mediterranean areas where riparian black poplar (*Populus nigra*) pollards are widespread but still understudied. First, the rapid rural depopulation has lead to the abandonment of pollarding creating trees with abundant, thick and heavy branches. Second, climate warming and alteration of river flows reduce soil moisture which could contribute to growth decline of riparian pollards. We investigated how these stress factors have impacted radial growth in seven sites located in four river basins of southern Aragón, north eastern Spain. We used dendrochronology to reconstruct the changes in radial growth during the period 1890–2020 and to assess how growth has responded to changes in temperature, precipitation and river flow variability. Since 1900 growth suppressions, probably corresponding to pollarding events, occurred in several decades (1910s, 1960s, 1980s and 1990s) and showed a high variability among sites and river basins. Suppressions peaked during the 1940s, probably associated to intense pollarding related to high timber and firewood demand after the Spanish Civil War. Poplar radial growth increased in response to high precipitation and river flow from March to April, particularly in sites located away of river banks. Pollarding abandonment and declines in soil moisture availability threaten the persistence of veteran black poplars. Active management through pollarding and protection should be implemented to preserve these iconic, anthropogenic woodlands due to their multiple ecological and cultural services.

1. Introduction

Society is demanding forest and woodland conservation and sustainable use, but we still lack historical and precise frameworks for differentiating natural vs. disturbed stages (Foster et al., 1996). Many forests across the northern hemisphere correspond to cultural landscapes which have been historically modified (Peterken, 1996; Rackam, 2006). For instance, forests across the Mediterranean Basin have been subjected to a secular history of use and management (Grove and Rackham, 2003). These forests and woodlands have been cleared, drastically altered and converted into croplands or grasslands, managed for timber or firewood or transformed through coppicing and pollarding (Bobiec et al., 2018). Nevertheless, we still lack adequate historical assessments on their past growth dynamics and accounts on their current status. Retrospective studies are fundament to forecast how these cultural, anthropogenic forests and woodlands will respond to the decline in their traditional management, climate warming and variability (Foster et al., 1996).

Pollarded stands of broadleaf species can harbor old trees which are able to store carbon as woody tissues or soil biomass for decades and represent important carbon reservoirs (Luyssaert et al., 2008). The regular cutting of pollarded trees allows them reaching much greater ages than uncut trees (Read, 2008). These singular stands also deliver unique cultural values (Rozas, 2004), and represent biodiversity hotspots since they provide habitats to many plant or animal species. For instance, hollow old oaks are unique habitats to rare, often threatened

* Corresponding author.
E-mail addresses: jjcamarero@ipe.csic.es (J.J. Camarero), ester.gonzalez@ipe.csic.es (E. González de Andrés), m.colangelo@ipe.csic.es (M. Colangelo), cdejaime@educa.aragon.es (C. de Jaime Loren).

https://doi.org/10.1016/j.foreco.2022.120268
Received 29 March 2022; Received in revised form 29 April 2022; Accepted 1 May 2022
Available online 9 May 2022

saproxylic beetle species (Ranius and Jansson, 2000), and pollarded ash trees are the habitats of rare epiphyte lichens and mosses (Moe and Botnen, 2000).

Pollarding of broadleaf species focused on obtaining wood and leaf fodder (Bargioni and Sulli, 1998). However, the intensity and frequency of traditional pollarding are declining and this technique has ceased in most places across Europe (Read, 2003). Therefore, we need suitable assessments of the situation of neglected pollarded stands to increase our ecological knowledge, promote their conservation and develop management politics to preserve them since they are a central part of the European cultural heritage. Currently, veteran pollards with abundant heavy branches or canopy dieback are widespread. Moreover, in addition to the ending of traditional pollarding these tree populations have to face the adverse effects of climate extremes as droughts which are key drivers of Mediterranean forest dynamics (Gazol et al., 2018).

In the historically grazed, seasonally dry and continental sites of eastern Spain (Teruel, Aragón), pollarded black poplar (*Populus nigra* L.) stands represented a unique source of wood and fodder for rural, local populations (De Jaime Loren and Herrero Loma, 2007). Here, the historical intensive use for sheep grazing and the harsh environmental conditions produced open landscapes dominated by grasslands and shrublands (Fig. 1). Near small rivers and streams, black poplars were planted, managed and pollarded in winter every 12–15 years, whereas grasslands were used for cattle illustrating the sustainable management of agro-forestry systems in climatically harsh environments (De Jaime Loren and Herrero Loma, 2007). Nowadays, these pollarded poplars are part of unique cultural landscapes, but they are menaced by the lack of management (traditional pollarding ceased in most sites after the 1960s; but see Fig. 1**c**). They also face additional stressors such as drought stress due to climate warming or lack of adequate soil moisture availability caused by river regulation (e.g., dam building) for agricultural uses (De Jaime Loren, 2017). Therefore, this is a special case of pollarded woodland because it is part of riparian ecosystems subjected to multiple stressors (Stella and Bendix, 2019).

In this study we followed a dendroecological approach to reconstruct past disturbance regimes (Lorimer and Frelich, 1989). In particular, we reconstructed the growth history of pollarded black poplar forests and woodlands in southern Aragón, north eastern Spain. We aimed: (i) to characterize the size and growth patterns of pollarded black poplars, (ii) to reconstruct growth history as related to changes in pollarding frequency and intensity, and (iii) to quantify the black poplar radial growth responses to climate variability and changes in river flow. We expected to detect peaks in growth suppressions during epochs with intense pollarding for timber or firewood extraction. We also hypothesized that pollarded trees located in the driest sites (e.g., far from river banks) will be the most sensitive to changes in growing-season precipitation and river flow.

2. Materials and methods

2.1. Study area

We selected seven sites in four river basins located in southern Aragón (Zaragoza and Teruel provinces, eastern Spain) where big, healthy pollarded poplar trees were found (Table 1, Fig. 2). In this area climate conditions are Mediterranean continental with dry summers and cold winters according to data from local climate stations (**Fig. S1**). Mean annual temperatures ranges 10.6–12.6 °C, with minimum values in January (mean temperature is 1.6–4.4 °C) and warmest conditions in July (mean temperature is 20.3–21.6 °C). Annual precipitation ranges 380–420 mm with peaks in May and autumn and low values in summer (July, August) and winter (January, February). In the study area, the

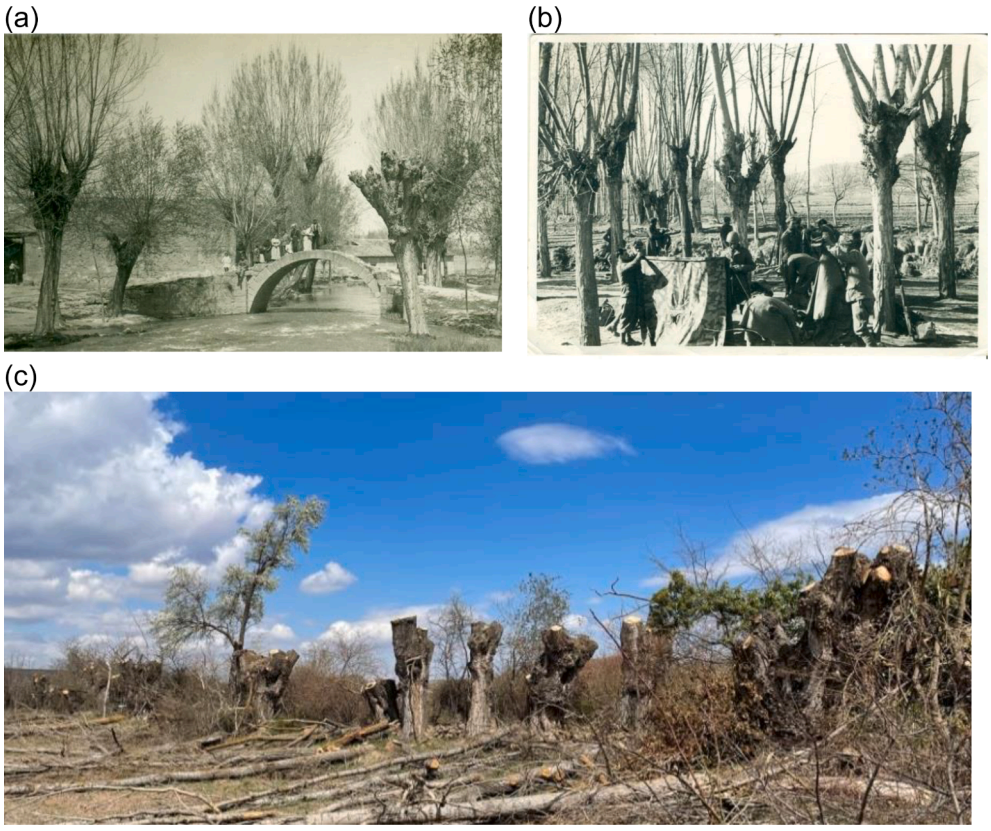

Fig. 1. Views of black poplars in old photographs taken near the Navarrete (a) and Fonfría (b) study sites and sampling site located in the (c) Allepuz study site (note the recently pollarded poplars whose branches were analysed). The images (a) and (b) were taken in the 1920s and late 1930s (soldiers correspond to the Spanish Civil War, which lasted from 1936 to 1939), respectively.

Table 1
Study sites and structural features. Values are means ± SE. Different letters indicate significant ($p < 0.05$) differences between sites based on Mann-Whitney U tests.

Site (code)	River basin	Flow data	Latitude (N)	Longitude (W)	Elevation (m a.s.l.)	Distance of sampled trees to nearest river bank (m)
Aguilar de Alfambra (AG)	Alfambra	X	40° 35′ 22′’	0° 48′ 01′’	1320	1.3 ± 0.6a
Allepuz (AL)	Alfambra	X	40° 30′ 28′’	0° 45′ 12′’	1328	30.0 ± 8.7c
Fonfría (FO)	Huerva		41° 00′ 42′’	1° 05′ 43′’	1192	1.5 ± 0.8a
Gúdar (GU)	Alfambra	X	40° 26′ 38′’	0° 43′ 57′’	1363	2.5 ± 0.8a
Huesa del Común (HU)	Aguasvivas		41° 00′ 49′’	0° 55′ 00′’	839	2.0 ± 0.7a
Marineta (MA)	Aguasvivas		41° 00′ 71′’	0° 57′ 37′’	868	6.9 ± 0.5b
Navarrete (NA)	Pancrudo	X	40° 55′ 55′’	1° 13′ 37′’	946	2.7 ± 0.9a

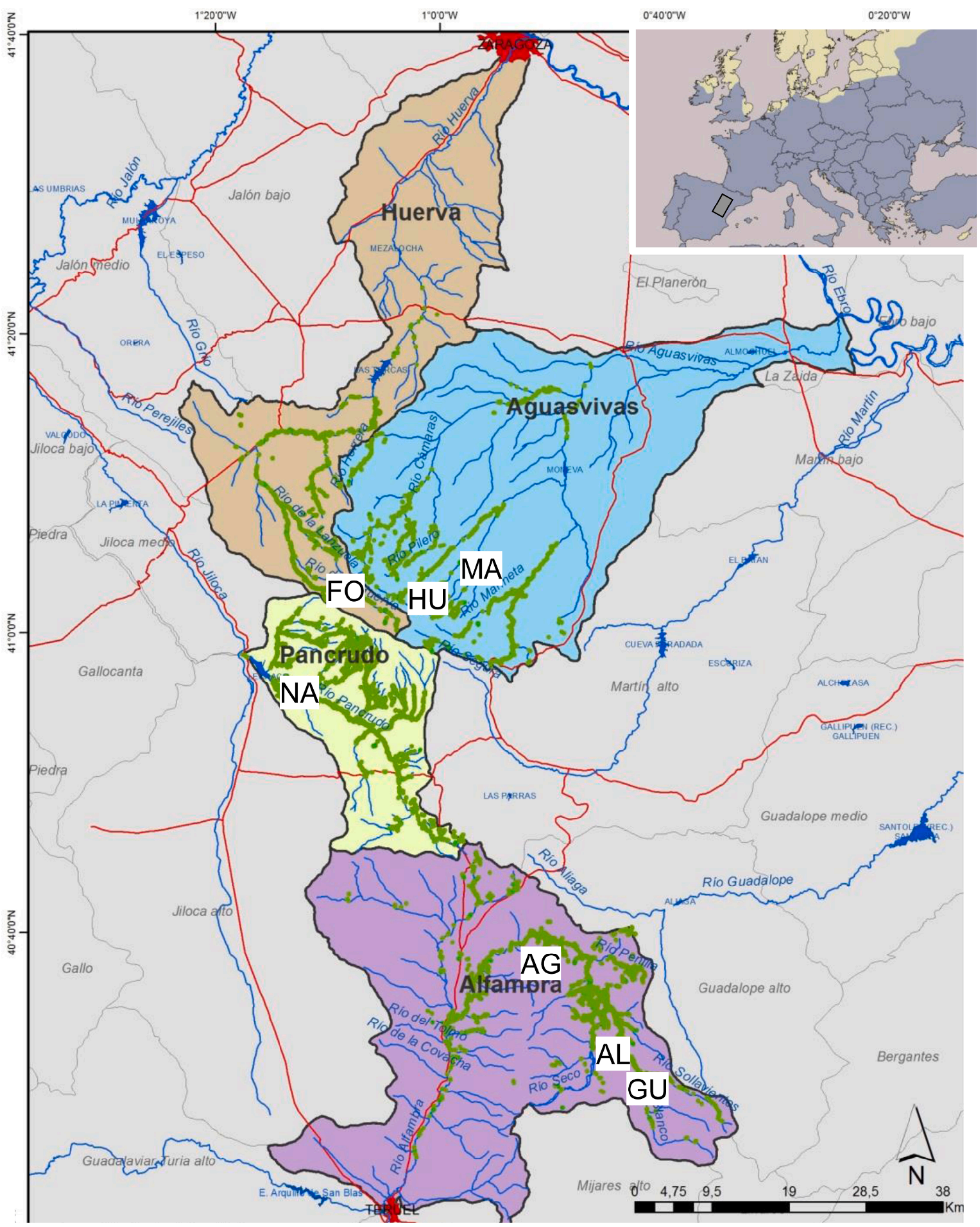

Fig. 2. Location of the study area and river basins in eastern Spain (the small map shows the distribution of black poplar in Europe and the location of the study area – grey box). In the map the seven study sites are indicated and different colors correspond to the studied river basins (from north to south): Huerva river (brown area), Aguasvivas river (blue area), Pancrudo river (yellow area) and Alfambra river (purple area). Blue lines and patches correspond to rivers and reservoirs, respectively. The red patches show Zaragoza and Teruel cities, Aragón region, north-eastern Spain. Green points indicate pollarded black poplars. (For interpretation of the references to colour in this figure legend, the reader is referred to the web version of this article.)

continentality degree is extreme for the Iberian Penisula, and some of the coldest temperatures for Spain (ca. −30 °C) have been recorded there (Aupí 2021).

In the study area, riparian vegetation in the wettest sites is dominated by black poplar, willows (*Salix atrocinerea* Brot., *Salix purpurea* L., *Salix alba* L., *Salix eleagnos* Scop.) and rush (*Juncus acutus* (L.) Torr. ex Retz) near the rivers and streams. Planted fruit trees are also frequent such as walnut (*Juglans regia* L.). In the nearby, drier locations the landscape is dominated by open grasslands and shrublands (*Crataegus monogyna* Jacq., *Rosa canina* L., *Amelanchier ovalis* Medik., *Genista scorpius* (L.) DC., *Thymus vulgaris* L., *Cistus laurifolius* L., *Ephedra* spp.) with scattered junipers (*Juniperus communis* L., *Juniperus phoenicea* L.). It is frequently observed that junipers recruit below poplars due to fruit dispersal and bird perching. In wetter, north- or north-west oriented slopes oaks are found (*Quercus ilex* L., *Quercus faginea* Lam.). Most sites have basic soils formed on limestones and marls, sometimes with

gypsum outcrops (Navarrete study site), and a few sites have acid soils (FO, Fonfría study site).

In the study sites, trees have not been pollarded for the past 20 years, excepting in the Navarrete site (Table 1) where half of sampled trees were pollarded 8 years ago. The lack of management of these forests is related to the rapid loss of rural population (Collantes and Pinilla, 2011) due to the massive migration to cities, which peaked in the 1960s (**Fig. S2**). Pollarding also declined because of the advances in building and heating technologies. In fact, the study area is located in the Iberian Range, which forms part of the so-called "Serranía Celtibérica", one of the most sparsely populated areas in Europe with mean density of 7 inhabitants km^{-2} (Burillo-Cuadrado et al. 2019).

2.2. Tree sampling

Sampling was done from autumn 2020 to spring 2021. In each site we selected dominant, pollarded black poplar trees and measured their diameter at 1.3 m, total height and pollarding height using tapes and a laser rangefinder (Nikon Forestry Pro 550 hypsometer). We also measured the distance between trees and the nearest river bank. We took two cores at 1.3 m from each tree using a Pressler increment borer. In addition, main branches were sampled in Allepuz (AL) and Gúdar (GU) sites at pollarding height (Fig. 1**c**, Table 2). These branches corresponded to the post-pollarding period. In all sites, sampled trees were located near river banks (Table 1). However, trees sampled in Marineta (MA) were not so close to the river bank and those in site AL were located away from the river and near a formerly used irrigation ditch. In contrast, trees in site GU were located close to the river. Therefore, we expected to find higher branch growth sensitivity to precipitation and river flow in the AL than in the GU site.

2.3. Climate and river flow data

Monthly mean temperature and precipitation data were obtained from the 0.1°-gridded E-OBS climate dataset (Cornes et al., 2018) since long and homogeneous climate records are scarce in the study area excepting in particular locations such as Daroca, Calamocha and Teruel climate stations (see **Fig. S1**). Using these climate data we calculated the Standardized Precipitation-Evapotranspiration Index (SPEI) (Vicente-Serrano et al., 2010). The SPEI quantifies drought length and severity at multiple temporal scales with values below −1.5 usually indicating severe drought. We calculated the SPEI for 1- to 48-month resolution.

We obtained three series of monthly flow data covering the period 1950–2017 and corresponding to the following stations: Navarrete del Río (Pancrudo river basin, 40° 55′ 53′'N, 1° 15′ 31′' W, 904 m), Villalba Alta (Alfambra river basin, 40° 36′ 56′'N, 0° 58′ 28′' W, 1060 m), and Teruel (Alfambra river basin, 40° 21′ 30′'N, 1° 07′ 13′' W, 885 m). River flow data were retrieved from the Spanish National Flow and Discharge Database ("Centro de Estudios y Experimentación de Obras Públicas", data available at the webpage https://ceh.cedex.es). According to these data, river flows peak from March to May and reach minimum values from July to September (**Fig. S3a**). This corresponds to a continental Mediterranean pluvial flow, which is characterized by maxima in spring and autumn–winter and a minimum in summer. In this regime, flow depends on precipitation and geological substrates of the study area such as limestones which can buffer the reduction of flow in summer (Solans and Poff, 2013). Annual flows vary between 15 and 40 hm^3, but they have declined in the study stations after peaking in the wet 1970s (**Fig. S3b**).

2.4. Tree-ring width data

Wood samples were air dried and carefully sanded following dendrochronological procedures until tree ring boundaries were visible (Fritts, 1976). Samples were scanned at 2400 dpi resolution and visually cross-dated. Then, ring widths were measured with a 0.001 mm resolution using scanned images and the CDendro software (Larsson and Larsson, 2018). The quality of cross-dating was checked using the COFECHA software which calculates moving correlations between individual series of ring-width values and the mean sites series (Holmes, 1983).

2.5. Tree-ring width processing

Since most cores did not have pith or innermost, curved rings, we did not use graphical methods to estimate age at 1.3 m. We assumed that stem chronological and geometric centers coincided. The length of missing radius was estimated as the difference between the geometric

Table 2
Structural features and radial growth data of sampled trees. In sites AL and GU branches (ALbr, GUbr) were also sampled and measured. Values are means ± SE. EPS is the Expressed Population Signal. Different letters indicate significant ($p < 0.05$) differences between sites based on Mann-Whitney *U* tests.

Site	Structural data			Tree-ring data							
	Dbh (cm)	Tree height (m)	Pollarding height (m)	No. trees (No. radii)	Age at 1.3 m (years)	Timespan	Ring width (mm)	First-order autocorrelation	Mean correlation with site series	EPS[#]	Negative growth change (%)[§]
AG	108.6 ± 8.0c	15.6 ± 1.5a	3.3 ± 0.2c	12 (24)	106 ± 12bc	1822–2020	2.79 ± 0.39b	0.63	0.34	0.59	19.6 ± 1.6a
AL	111.6 ± 15.5c	27.4 ± 1.7c	2.8 ± 0.2b	10 (20)	99 ± 10b	1877–2020	3.05 ± 0.45b	0.65	0.49	0.82	25.2 ± 2.4b
FO	72.3 ± 6.9b	19.0 ± 1.0b	2.8 ± 0.1b	23 (46)	90 ± 4a	1888–2020	3.34 ± 0.35b	0.72	0.57	0.84	42.5 ± 4.1d
GU	118.3 ± 9.9c	19.1 ± 1.1b	2.4 ± 0.1a	12 (24)	82 ± 5a	1910–2020	2.93 ± 0.38b	0.69	0.47	0.81	33.4 ± 3.6c
HU	60.3 ± 1.3a	15.6 ± 1.3a	2.1 ± 0.2a	5 (10)	103 ± 15bc	1877–2020	1.64 ± 0.39a	0.62	0.36	0.61	39.8 ± 4.2 cd
MA	81.5 ± 4.9b	14.0 ± 0.3a	3.0 ± 0.1b	16 (32)	91 ± 5a	1886–2020	2.32 ± 0.31a	0.53	0.40	0.76	34.5 ± 3.3c
NA	76.1 ± 4.0b	15.6 ± 1.8a	3.4 ± 0.1c	22 (44)	128 ± 14bc	1794–2020	1.71 ± 0.24a	0.65	0.38	0.79	15.4 ± 1.4a
ALbr	–	–	–	7 (14)	54 ± 1[¥]	1961–2020	3.03 ± 0.59b	0.74	0.59	0.88	–
GUbr	–	–	–	10 (20)	57 ± 1[¥]	1948–2020	3.56 ± 0.47b	0.78	0.48	0.76	–

[#] Calculated for the common period 1970–2020.
[§] Calculated for the common period 1890–2020.
[¥] Age of branches sampled at pollarding height.

radius, after removing bark thickness, and the total core length following (Norton et al., 1987). Then, the number of inner missing rings was estimated by extrapolating the mean radial growth rate from the innermost 10 rings (Rozas 2003, 2004).

To estimate periods of growth suppression, which could be attributed to past pollarding (cf. Rozas, 2004), we calculated negative growth changes (NGC) following Nowacki and Abrams (1997):

$$NGC = [(M1 - -M2)/M2] \times 100 \quad (1)$$

where M1 and M2 are previous and subsequent 10-year ring-width medians calculated on individual series and shifted every year (**Fig. S4**). We considered a 50% threshold in NGC observed in at least 50% of trees in each site for defining major growth suppressions, whereas a 25%-threshold in at least 50% of trees was regarded as moderate suppressions. The NGC series were obtained for the common period 1890–2020, i.e. they were plotted for the 1900–2010 period. Analogously, we also calculated positive growth changes (PGC) and estimated the number of major and moderate releases following:

$$PGC = [(M2 - -M1)/M1] \times 100 \quad (1)$$

Both NGC and PGC were calculated on cores' ring-width series but not on branches' series since these cross-sections corresponded to the period after the last pollarding was done about 55 years ago (see Table 2). Finally, we calculated Spearman correlations between sites' mean series of NGCs or PGCs to assess among-site similarity in growth suppressions or releases, respectively.

To study growth responses to climate after removing size-, ontogeny- or disturbance-related trends, we detrended tree-ring width series. We selected cubic smooth spline with a length of 0.67 of the series and a 0.5 response cut-off. Then, observed values were divided by fitted values to obtain ring-width indices. Indexed series were subjected to pre-whitening to remove temporal autocorrelation and then averaged using bi-weight robust averages to obtain pre-whitened, residual chronologies. To assess within-site growth coherence we calculated the mean correlation of the individual series with the mean site series. We also calculated the Expressed Population Signal (EPS) for the common, best-replicated period 1970–2020. The EPS was used to assess how replicated and coherent was each site series or chronology (Wigley et al., 1984). To characterize and compare the site series or ring-width data, we calculated the ring width and the first-order autocorrelation which measures year-to-year growth persistence (Fritts, 1976).

2.6. Statistical analyses

To compare individual linear growth (ring-width) trends among sites considering the period 1990–2020 we used the Kruskall-Wallis test followed by paired Mann-Whitney tests. To evaluate the relationships among sites' series of ring-width indices we calculated a Principal Component Analysis (PCA) on the covariance matrix considering cores' and branches' indices for the common and best-replicated period 1970–2020. We kept the first (PC1) and second (PC2) principal components because they individually accounted for at least 15% of variance.

The relationships between the sites' series of ring-width indices vs. monthly climate (mean maximum and minimum temperatures, total precipitation), SPEI and flow data were based on Pearson correlations. Correlations were calculated for the period 1950–2020 in the case of stem cores and for the period 1970–2020 in the case of branches data. Correlations were obtained from prior October (year previous to the year of tree-ring formation) to current September when the late growing season occurs. To assess the temporal stability between growth indices and selected precipitation or flow data we calculated 20-year moving correlations between these series.

All analyses were performed in the R environment for statistical computing (R Development Core Team, 2021). The package dplR (Bunn, 2010; Bunn et al., 2021) was used to detrend and analyse tree-ring width series, the package TRADER was used to calculate NGCs and PGCs (Altman et al., 2014), and the Kruskall-Wallis test, the SPEI was calculated using the R package SPEI (Beguería et al., 2014), the PCA and climate-growth relationships (correlations) were calculated using the PAST ver. 4.0 software (Hammer et al., 2001).

3. Results

3.1. Size and age of pollarded trees

The mean diameter of all sampled poplars was 87.5 cm (range 39.3–196.0 cm), their mean height was 16.8 m (range 6.7–35.0 m) and the mean pollarding height was 2.9 m (range 1.5–4.8 m; Table 2). The trees with thickest stems were found in Aguilar de Alfambra (AG), Allepuz (AL) and Gúdar (GU) sites and the highest individuals were found in the AL site. The highest mean pollarding height (3.3–3.4 m) was found in AG and Navarrete (NA) sites, and the lowest (2.2–2.4 m) in GU and Huesa del Común (HU) sites. Tree diameter and height were positively related (Fig. 3**a**), whereas tree height and pollarding height were negatively related (Fig. 3**b**).

The oldest sampled individuals were found in the NA (227 years) and AG (198 years) sites. The NA site can be considered an old-growth stand with nine out of twenty two sampled trees (41%) having ages over 200

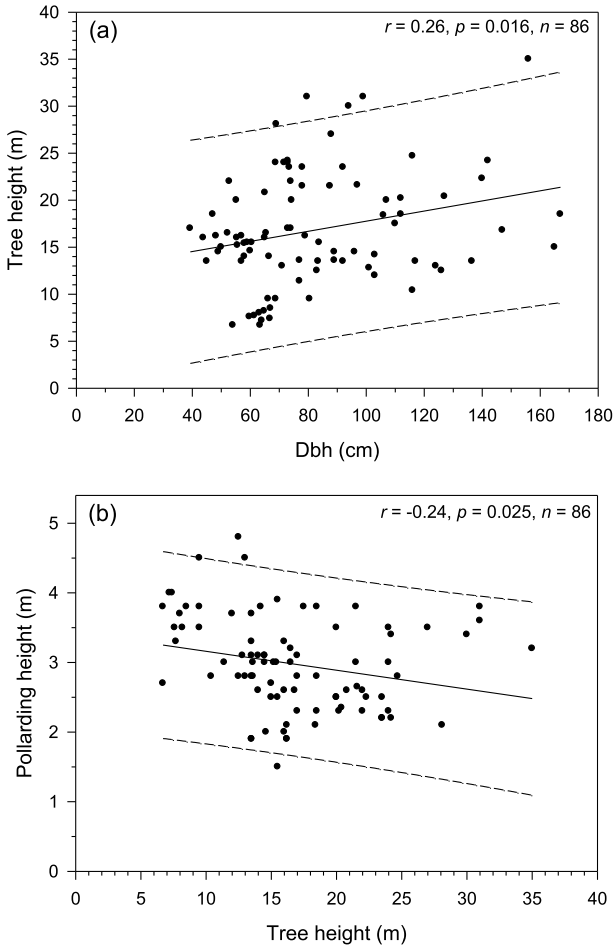

Fig. 3. Main structural characteristics of the sampled pollarded black poplar trees: (a) positive relationship between diameter at breast height (Dbh) and tree height, and (b) negative relationship between tree height and pollarding height. Statistics corresponding to linear regressions (continuous lines) are shown in the upper right corner of each plot. The dashed lines show the 95% prediction intervals.

years. The age of branches sampled in sites AL and GU was very uniform (54–57 years; see Table 2 and Fig. 4).

3.2. Growth patterns and trends

The highest mean growth rates were found in AL and FO sites (3.05–3.34 mm), whilst the lowest rates corresponded to HU and NA sites (1.64–1.71 mm). The series from MA and HU sites showed the lowest first-order autocorrelation values, whereas branches' series showed the highest values followed by FO and GU trees' series (Table 2). The highest mean NGCs were found in FO and HU sites, whereas the lowest values were found in NA and AG sites.

According to the Kruskall-Wallis tests, there were significant differences among sites regarding individual growth trends for the period 1990–2020 ($H = 46.76$, $p < 0.001$). All sites presented mean negative growth trends with lowest values (mean ± SE) for sites FO (-0.006 ± 0.001 mm yr^{-1}), AG (-0.005 ± 0.001 mm yr^{-1}), GU and HU (both (-0.004 ± 0.001 mm yr^{-1}). In contrast, NA (0.002 ± 0.001 mm yr^{-1}), AL and MA (both 0.001 ± 0.001 mm yr^{-1}) sites presented positive trends. As expected, branches' series also presented negative trends (both sites, −0.005 ± 0.001 mm yr^{-1}).

Overall, the 1890–2020 period was well replicated considering all sites (Fig. 4), albeit the EPS values were usually below the 0.85-threshold often considered in tree-ring studies during the common period 1970–2020 (Table 2). The highest EPS values were found for the FO (0.84), AL (0.82) and GU (0.81) sites. These sites also showed the highest mean correlations of individual series with site series. The lowest EPS values corresponded to AG (0.59) and HU (0.61) sites. The only mean series or chronology with EPS above the aforementioned threshold corresponded to the branches from site AL with an EPS of 0.88, confirming a high coherence of that series. Branches showed high mean correlations of individual series with site series.

3.3. Growth changes as proxies of pollarding

The NGCs peaked in the 1910s in sites AG and NA, and from the late

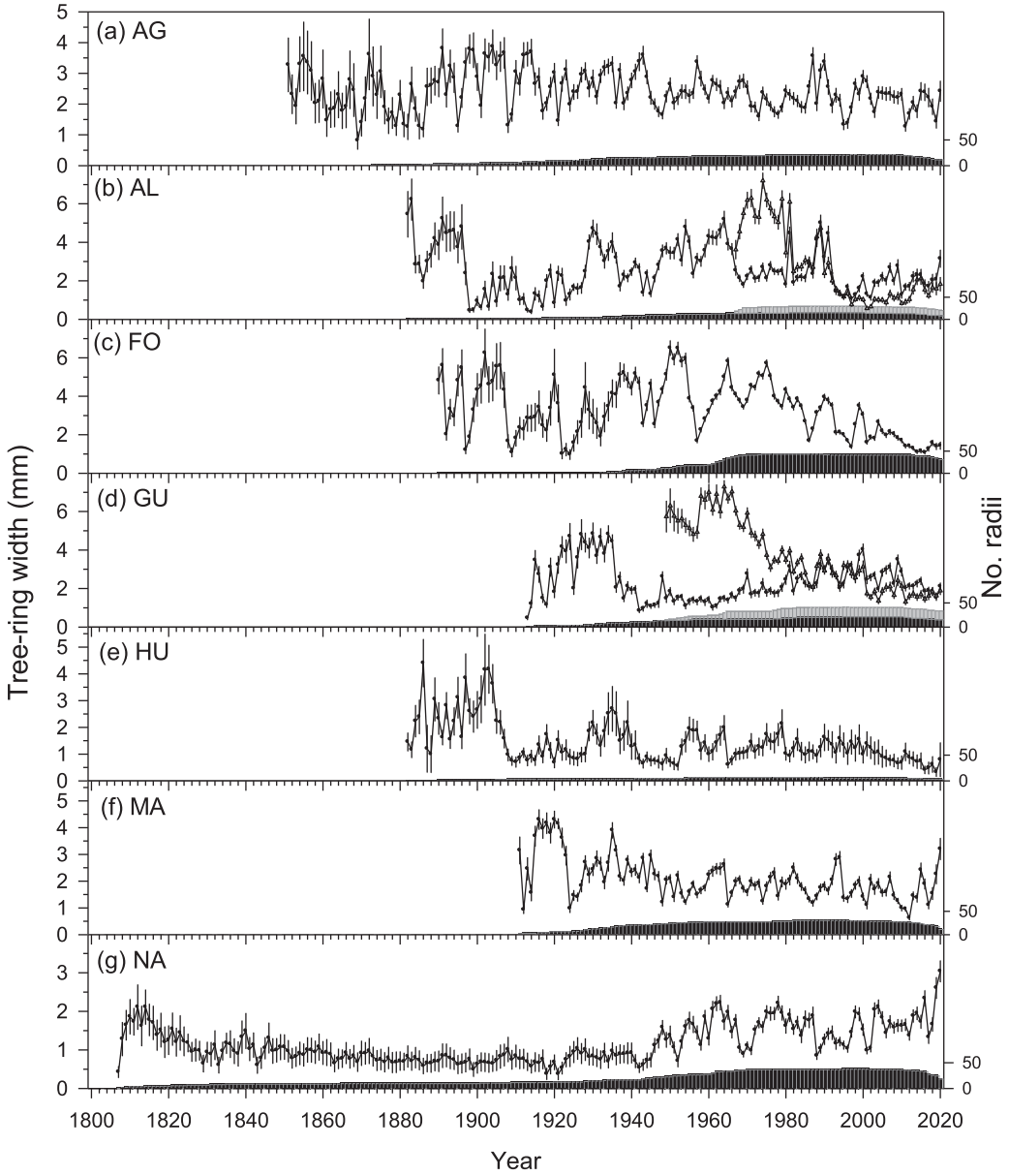

Fig. 4. Growth data of black poplars based on the mean series of tree-ring width calculated for each site. Growth data were obtained for stem cores (black bars) and branches cross-sections (grey bars) in sites AL and GU. Values are means ± SE. The bars show the annual number of measured radii (right y axes) with black and grey fills corresponding to stem and branch radii, respectively.

1930s to early 1940s in sites AL, FO, GU, HU and MA (Fig. 5). In sites AL and NA, other NGCs peaks were observed in the mid to late 1960s and from the late 1980s to early 1990s. In sites FO and HU, NGCs also increased in the 2000s. There was a high number of moderate and major suppressions in the early 1920s, early 1950s, mid 1970s and late 1990s. Regarding the PGCs, they peaked from the late 1970s to early 1980s in sites AG, AL, MA and NA (**Fig. S5**). Previous peaks were also detected in the 1920s (sites AL, GU, HU and NA), 1940s (sites AL, FO and NA), 1950s (sites AG, HU, MA and NA) and from the 1960s to the 1970s in sites GU and HU. There was a high number of moderate and major releases in the mid-1920s, early 1950s, mid-1970s and late 1990s.

The NGCs series of sites FO, GU, HU and MA were positively related, showing all them the NGC peaks in the late 1930s to early 1940s (Table 3). The sites FO, HU and MA were located nearby (Fig. 2). The PGCs series of sites AG, FO, GU, HU, AL and MA were positively related (Table 3).

Table 3
Spearman correlations calculated between the site's series of negative (values shown above the diagonal) and positive (values shown below the diagonal) growth changes considering the common period 1890–2020. Significant ($p < 0.05$) values are shown in bold. See sites' codes in Table 1.

	AG	AL	FO	GU	HU	MA	NA
AG		**0.27**	−0.12	−0.13	0.12	0.18	**−0.21**
AL	0.12		−0.07	**−0.36**	0.15	**−0.24**	**0.32**
FO	**0.28**	−0.11		**0.50**	**0.55**	**0.23**	0.13
GU	**0.33**	**−0.28**	**0.61**		**0.45**	**0.61**	−0.18
HU	**0.46**	**0.31**	**0.56**	**0.43**		**0.25**	0.09
MA	**0.62**	**−0.34**	**0.33**	**0.60**	**0.25**		−0.12
NA	0.03	**0.46**	0.09	−0.06	0.13	−0.01	

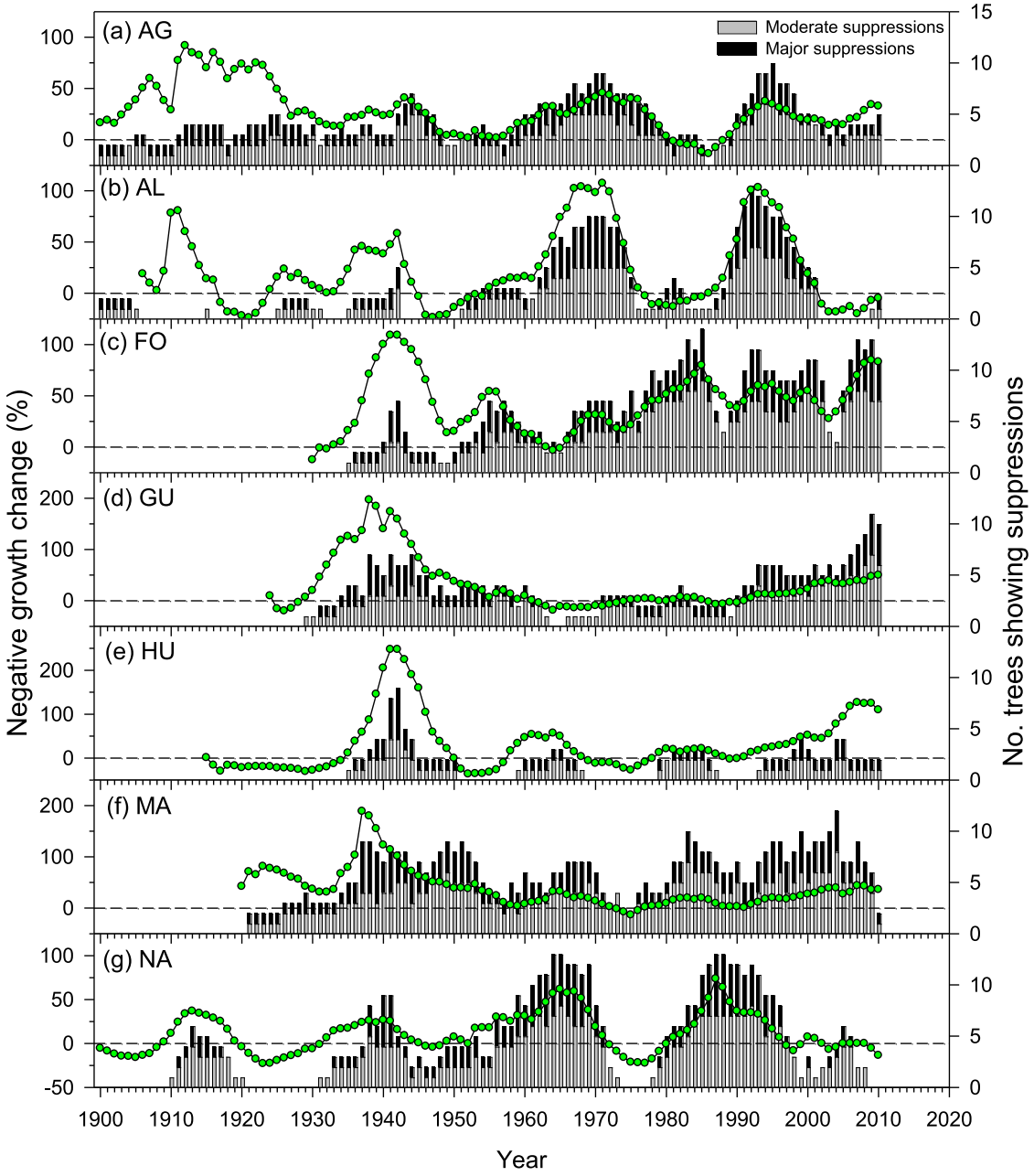

Fig. 5. Series of negative growth changes showing potential pollarding events corresponding to severe growth reductions (high values of negative growth change) and number of trees showing moderate (grey bars) and major (black bars) growth suppressions (right y axes).

3.4. Growth responses to climate, drought and river flow variability

We obtained series of ring-width indices for stem cores and branches cross-sections covering the 1950–2020 and 1970–2020 periods, respectively (**Fig. S6**). The PCA showed that series of the nearby MA, HU, FO, NA and AG sites (see Fig. 2) were aligned along the PC1, which accounted for 36.1% of the total variance, whereas core and branches series of the southern AL and GU sites were aligned along the PC2, which accounted for 19.8% of the variance (**Fig. S7**). Some years were highlighted by the PCA showing very low PC1 scores and corresponding to low growth rates such as 1986, 1995–1996, 2005 and 2012 (Fig. 6), whilst high rates were found in 2020 and 1979 (**Fig. S5**). In sites AL and GU, growth rates were high in 1988–1989 and very low in 1982, 2001 and 1990. In these two sites, correlations between stem and branch series of ring-width indices were highly significant ($p < 0.001$) in the AL ($r = 0.78$) and GU ($r = 0.83$) sites considering the common period 1970–2020.

Considering the indexed series from nearby sites MA, HU, FO, NA and AG we found that poplar growth rates were not very responsive to climate variability (**Fig. S8**). In addition, responses changed among sites. We found positive correlations between MA ring-width indices and winter maximum temperatures and March-April precipitation. In AG there was a positive correlation between indices and prior October minimum temperatures, but a negative correlation with September minimum temperatures in NA. In FO, indices responded negatively to high January minimum temperatures and elevated prior November precipitation.

We found more and stronger correlations between ring-width indices from branches and river flow as compared to precipitation in site AL (**Fig. S9**). Branch radial growth was enhanced by high precipitation and river flow from March to April (Figs. 6 and 7). High flow from May to June also improved growth. In site AL, stem radial growth was also enhanced by high March ($r = 0.24$) and April ($r = 0.28$) precipitation and elevated April ($r = 0.25$) and June river flow ($r = 0.29$), whereas no significant correlation was found between growth indices from cores and temperature, precipitation or flow data in site GU. However, branch growth indices and September flow were positively related in this site (**Figs. 7 and S9**).

We only found significant ($p < 0.05$) correlations between ring-width indices and SPEI values in the FO and AL sites. In site FO the highest correlation ($r = 0.41$) was found for 45-month May SPEI, whereas in site AL the highest correlation ($r = 0.31$) was found for 2-month April SPEI. Interestingly, this correlation was similar for cores and branches from site AL ($r = 0.48$) when considering the same common period for both cores and branches (1961–2020).

The associations between branch growth indices and April precipitation or flow in the responsive site AL were strong but not stable through time (**Fig. S10**). They peaked from the mid to late 1980s in the case of precipitation and in the 1990s in the case of river flow. However, correlations declined, particularly in the case of flow, in the 2000s. After removing the influence of precipitation on flow, we still found the same weakening in growth-flow correlations confirming this was due to flow reductions rather than to a decline in precipitation (**Fig. S3b**).

4. Discussion

We found a peak in growth reductions (negative growth change) during the 1940s in five out of seven sites. Such marked and lasting growth declines could be attributed to pollarding (cf. Rozas 2004). We also detected that growth of pollarded trees located in drought-prone sites such as MA, where trees were found far from river banks, and AL, where trees were found near a formerly used irrigation ditch, was sensitive to changes in March to April precipitation and river flow. The different growth trends observed among sites after 1990, when climate became particularly warmer in the study area, suggest different future dynamics. For instance, it could be expected that sites with the most negative growth trends and very responsive to drought (e.g., site FO) could become more vulnerable or loss vitality as compared with sites with positive growth trends (e.g., site NA).

4.1. Growth history of pollarded poplars

In the study region there was a demographic surge in the 1940s. The increase of coal price after World War I, the economic legacies of the Spanish Civil War (1936–1939) and the autarky politics of the subsequent dictatorship lead to an increase in the use and demand of firewood during the 1940s (Infante-Amate and Iriarte-Goñi, 2017). According to these authors, the firewood consumption rate in the study area (about 5 kg hab^{-1} day^{-1}) was among the highest in Spain from the 1930s until 1955 and rapidly declined afterwards when fossil fuels became widely used, rural electrification extended and population massively migrated to cities. The local timber demand also increased after the Spanish Civil War for rebuilding or restoring damaged or destroyed rural houses, barns and corrals using poplar beams since one of the Spanish Civil War front lines was established in the study area severely affecting villages' infrastructures during one year (De Jaime Loren and Herrero Loma,

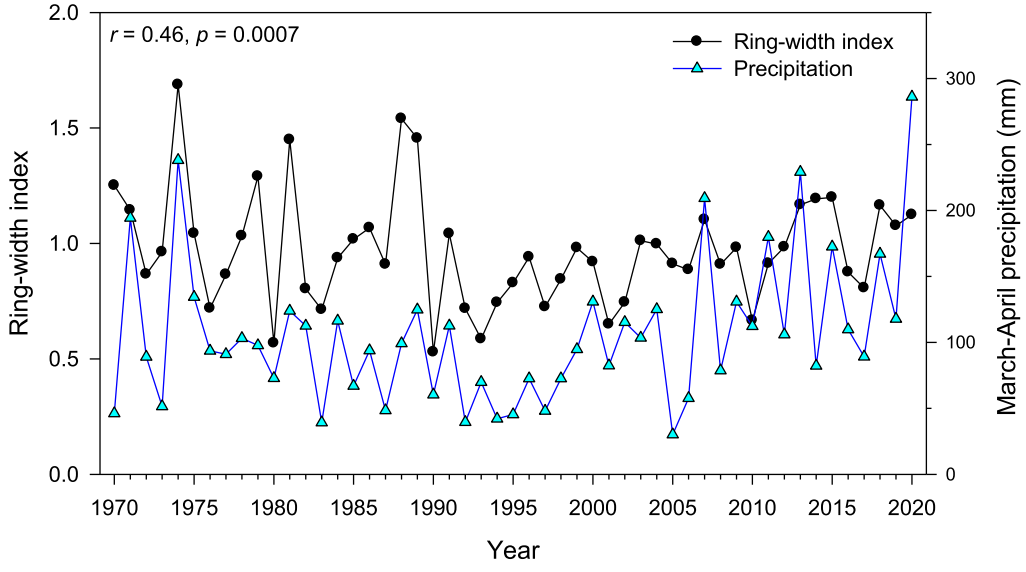

Fig. 6. Growth rates in poplar branches increased as March to April precipitation did as shown by the positive correlation found between both variables in AL site.

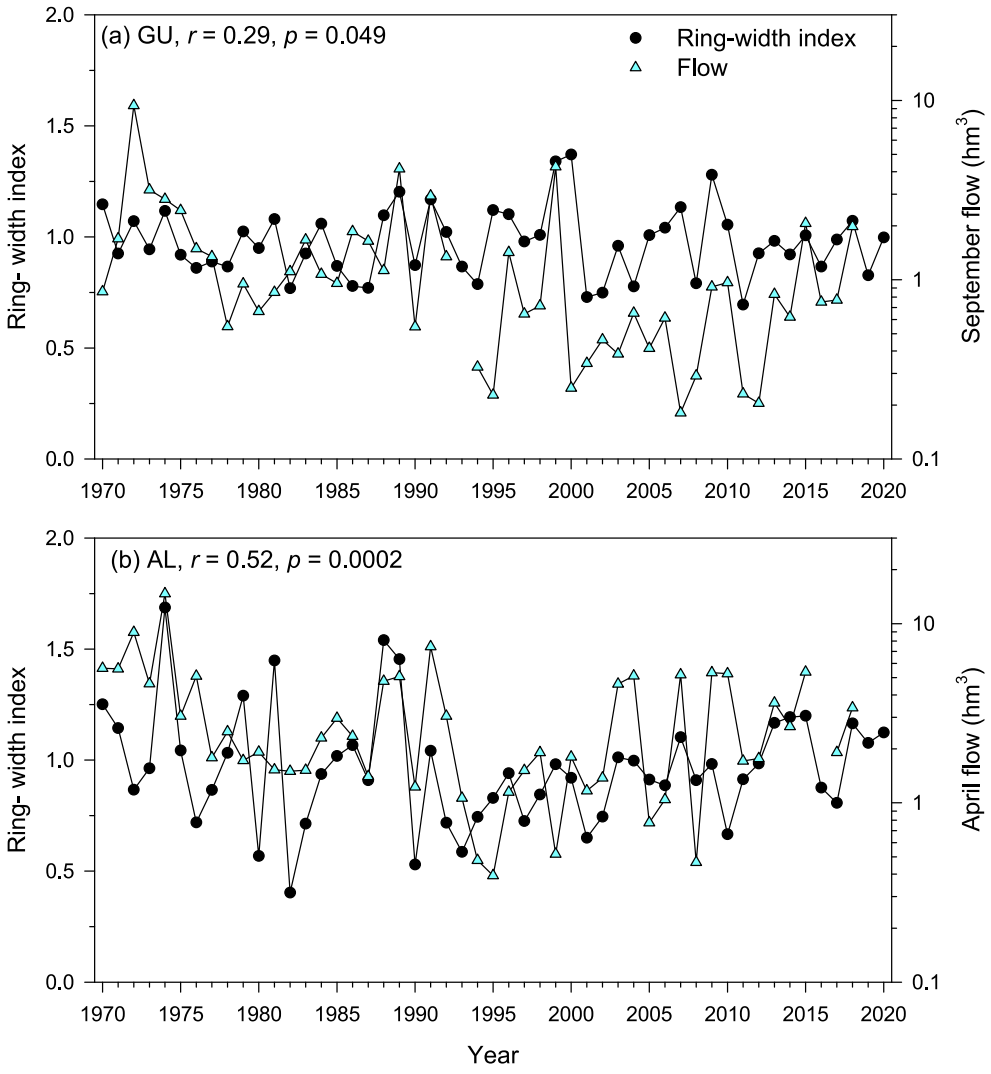

Fig. 7. Poplar branch radial growth rates and river flow were positively associated as shown the positive correlations found between both variables in GU (a) and AL (b) sites. Note the logarithmic scales of monthly flow data corresponding to the Teruel station in the Alfambra river.

2007). Such historical changes could explain the peak in pollarding intensity of the study poplar sites driven by the increased demand of local timber and firewood. Growth suppressions were also observed in the 1960s, 1980s and 1990s, but the negative growth change never reached the intensity observed in the 1940s. Such considerable rural migration to cities during the 20th century affected most European countries, but the depopulation rate was exceptionally high in some Spanish regions (Collantes and Pinilla, 2021). Some of these areas contain most black poplar pollards (e.g., Teruel province) which explains their current vulnerability since pollarding was tightly linked to rural populations and timber or wood extraction (De Jaime Loren and Herrero Loma, 2007).

4.2. Growth responses to climate and river flow

Poplars are phreatophyte species. In the case of black poplar, its growth mainly depends on phreatic water and declines when water tables are suppressed (Sánchez-Pérez et al., 2008; Singer et al. 2013; 2014). Water shortage leads to branch abscission, canopy dieback, growth decline and even mortality in riparian poplar species (Scott et al., 1999; Rood et al., 2000; 2007). These features support our correlation analyses showing a tight connection between radial growth of pollarded poplars and March-April precipitation and river flow. These responses were found in sites subjected to fluctuating water tables either far from river banks (e.g., site MA) or near formerly used irrigation ditches (e.g., site AL). In the study area, dry spring to summer conditions correspond to warmer temperatures and lower-than-normal precipitation (Gazol et al., 2018), which reduce the quantity of runoff contributing to river discharge (Solans and Poff, 2013). Since branch growth was not so affected by pollarding as stem growth, branches showed stronger responses to precipitation and flow variability than stems. The branch responsiveness to climate and flow changed through time because branch growth decoupled from river flow from the 2000s onwards. Such weakening was not probably due to competition among branches, but to severe and persistent flow reduction (**Fig. S3b**), often associated to unsustainable river management due to agricultural water demand (De Jaime Loren and Herrero Loma, 2007).

We found that annual precipitation and river flow became decoupled from the late 1990s to early 2000s as river flow decreased (**Figs. S3b, S11**). Since annual precipitation showed no significant trend from 1950 to 2020 and April precipitation showed a positive trend (Kendall $\tau = 0.18$, $p = 0.02$), the negative tendency of river flow may be explained by climate warming. In fact, annual temperature has significantly increased in the study area ($\tau = 0.44$, $p < 0.001$). Particularly, we found that maximum April temperature has increased ($\tau = 0.29$, $p < 0.001$). This could lead to a higher evaporative demand and explain the negative association with growth observed in some sites such as FO. In fact, black poplar is characterized by high sap flow rate and canopy water evaporative demand (Lambs and Muller, 2002; Sánchez-Pérez et al., 2008).

Therefore, forecasted warmer and drier conditions and reduced flow of shallow phreatic water due to water extraction, river damming or ditch abandonment could contribute to the decline of many riparian pollarded poplars (cf. Amlin and Rood, 2003; Lambs et al. 2006). In drought-prone sites, poplars could have adapted to variable phreatic water supply by growing more shallow roots and using several water sources but this should be investigated in sites with old individuals (e.g., NA site) using water and wood H, C and O isotopes.

4.3. Implications for black poplar pollard management and conservation

We found large and old pollarded poplars, particularly in the AL, NA, HU and AG sites, with several trees reaching ages over 200 years. This age estimate is close to the maximum ages (250–350 years) estimated for old, non-pollarded black poplars (Turok et al., 1997). The existence of large, old trees with relatively good vitality suggests further pollarding should be applied to preserve these healthy trees, which rarely presented rotten heartwood. We acknowledge this observation may be biased because our sampling focused on apparently healthy trees. These massive and often ancient trees are exceptional poplars which could be catalogued and protected as monumental trees. They represent valuable remains of pollarded woodlands, constitute unique long-term carbon pools (Luyssaert et al., 2008) and biodiversity hotspots, provide cultural and eco-touristic goods and services and are also reservoirs of native genotypes less influenced by artificially selection than younger, imported poplar stocks (Cottrell et al., 2002). In addition, the study populations are located near the southern limit of the species distribution area and could provide drought-adapted genotypes.

Pollarded veteran trees and woodlands are human-made, iconic components of European landscapes and require adequate conservation and active management measures to reverse or slow down their decline (Read 1996, 2000). Traditional pollarding techniques of black poplars, with 20–40 year long pollarding cycles, should be taught to farmers, foresters, land owners and managers by adapting them to current technological advances and incorporating them into modern land management systems. Planting local genotypes or favoring natural regeneration should be also done. These management techniques are more expensive than no intervention but they should be carried out and kept running once started. Designation of suitable areas with pollards as nature reserves where pollarding is maintained, as is the case of the AG site, should also involve local stakeholders. This would help to better interpret pollards as components of cultural landscapes and highlight the cultural and historical values of similar traditional agro-forestry systems.

According to Read (2003), we must overcome the prejudice that nature conservation depends on rare, wild undisturbed areas and realize that manmade landscapes such as pollarded woodlands provide unique conservation values and require human intervention. Pollarded trees are part of Europe's heritage and their conservation should be explicitly considered by agricultural policies providing subsidies to local farmers and reverting or stopping rural depopulation. At regional to national scale, the river basin management agencies ("Confederación Hidrográfica") and regional environmental agencies should collaborate and actively participate to catalogue and preserve these riparian systems.

In general, the greenness of riparian vegetation is more coupled to groundwater along streams with natural flow regimes compared with streams altered by human impacts (Rohde et al., 2021; Šenfeldr et al., 2021). Again, river basin management agencies should monitor and keep ecological river flows given the high dependency of black poplar growth on phreatic water use and the elevated demand of water by farmers in drought-prone Mediterranean regions and under a context of climate warming.

5. Conclusions

Historical peaks in growth reductions of pollarded black poplars during the 1940s corresponded to an increase in the demand of timber and firewood by rural populations. Poplar radial growth was constrained by low precipitation and reduced river flow from March to April, particularly in sites where the availability of phreatic water most fluctuated. To understand if poplar growth is becoming increasingly constrained by the decline in river flows, further studies could investigate the H, C and O isotopic signatures of water and wood. This would allow linking the changes in water availability to stem radial growth.

Pollarded black poplar woodlands represent understudied, man-made, iconic landscapes with high ecological and cultural values. They face a declining trend if pollarding techniques are no longer applied and river flows are reduced due to climate warming and increased water demand for agriculture and farming. If pollarding practices are not carried out, many old trees, often at least 200 years old, could collapse leading to the decline or extinction of some poplar populations and cascading on other organisms feeding on or inhabiting these veteran poplars. Active management of these anthropogenic, rural landscapes is mandatory and urgent because they illustrate how humans have shaped European agro-forestry ecosystems for millennia.

CRediT authorship contribution statement

J. Julio Camarero: Conceptualization, Formal analysis, Funding acquisition, Writing – original draft. **Ester González de Andrés:** Data curation, Methodology, Writing – original draft, Writing – review & editing. **Michele Colangelo:** Data curation, Methodology, Writing – original draft, Writing – review & editing. **Chabier de Jaime Loren:** Conceptualization, Investigation, Writing – review & editing.

Declaration of Competing Interest

The authors declare that they have no known competing financial interests or personal relationships that could have appeared to influence the work reported in this paper.

Acknowledgements

This study was supported by project FORMAL (RTI2018-096884-B-C31) from the Spanish Ministry of Science and Innovation. We acknowledge the E-OBS dataset from the EU-FP6 project UERRA (http://www.uerra.eu) and the Copernicus Climate Change Service, and the data providers in the ECA&D project (https://www.ecad.eu). We thank the editor and two anonymous reviewers for their constructive comments.

Appendix A. Supplementary material

Supplementary data to this article can be found online at https://doi.org/10.1016/j.foreco.2022.120268.

References

Altman, J., Fibich, P., Dolezal, J., Aakala, T., 2014. TRADER: A package for tree ring analysis of disturbance events in R. Dendrochronologia 32 (2), 107–112.
Amlin, N.M., Rood, S.B., 2003. Drought stress and recovery of riparian cottonwoods due to water table alteration along Willow Creek, Alberta, Trees Struct. Funct. 17, 351–358.
Aupí, V., 2021. El triángulo de Hielo. Dobleuve Eds. Teruel, Spain.
Bargioni, E., Sulli, A.Z., 1998. The production of fodder trees in Valdagno, Vicenza, Italy. In: Kirby, K.J., Watkins, C. (Eds.), The Ecological History of European Forests. CAB International, New York, pp. 43–52.
Beguería, S., Vicente-Serrano, S.M., Reig, F., Latorre, B., 2014. Standardized precipitation evapotranspiration index (SPEI) revisited: parameter fitting, evapotranspiration models, tools, datasets and drought monitoring. Int. J. Climatol. 34 (10), 3001–3023.

Bobiec, A., Reif, A., Öllerer, K., 2018. Seeing the oakscape beyond the forest: a landscape approach to the oak regeneration in Europe. Landsc. Ecol. 33 (4), 513–528.
Bunn, A.G., 2010. Statistical and visual crossdating in R using the dplR library. Dendrochronologia 28 (4), 251–258.
Bunn, A., Korpela, M., Biondi, F., Campelo, F., Mérian, P., Qeadan, F., Zang, C., 2021. dplR: Dendrochronology Program Library in R. R package version 1.7.2. https://CRAN.R-project.org/package=dplR.
Burillo-Cuadrado, M.P., Rubio Terrado, P., Burillo Mozota, F., 2019. Strategies facing the depopulation of the Serrania Celtibérica within the framework of the European cohesion policy 2021–2027. Economía Agraria y Recursos Naturales 19, 83–97.
Collantes, F., Pinilla, V., 2011. Peaceful Surrender: The Depopulation of Rural Spain in the Twentieth Century. Cambridge Scholars Publishing.
Cottrell, J.E., Munro, R.C., Tabbener, H.E., Gillies, A.C.M., Forrest, G.I., Deans, J.D., Lowe, A.J., 2002. Distribution of chloroplast DNA variation in British oaks (*Quercus robur* and *Q. petraea*): the influence of postglacial colonisation and human management. For. Ecol. Manage. 156 (1-3), 181–195.
De Jaime Loren, F.C., 2017. Distribución geográfica, estimación de la población y caracterización de las masas de chopo cabecero en las cuencas del Aguasvivas, Alfambra, Huerva y Pancrudo. University of Zaragoza, Spain. PhD Thesis.
De Jaime Loren, F.C., Herrero Loma, F. 2007. El chopo cabecero en el sur de Aragón. La identidad de un paisaje. Centro de Estudios del Jiloca, Calamocha, Spain.
Foster, D.R., Orwlg, D.A., McLachlan, J.S., 1996. Ecological and conservation insights from reconstructive studies of temperate old-growth forests. Trends Ecol. Evol. 11 (10), 419–424.
Fritts, H.C., 1976. Tree Rings and Climate. Academic Press, London, UK.
Gazol, A., Camarero, J.J., Vicente-Serrano, S.M., Sánchez-Salguero, R., Gutiérrez, E., De Luis, M. et al., 2018. Forest resilience to drought varies across biomes. Glob. Chang. Biol. 24, 2143–2158.
Grove, A.T., Rackham, O., 2003. The Nature of Mediterranean Europe: An Ecological History. Yale University Press, New Haven, UK.
Hammer, Ø., Harper, D.A.T., Ryan, P.D., 2001. PAST: Paleontological Statistics Software Package for Education and Data Analysis. Palaeontologia Electronica 4, 9 pp.
Holmes, R., 1983. Computer-assisted quality control in tree-ring dating and measurement. Tree Ring Bull. 43, 69–78.
Infante-Amate, J., Iriarte-Goñi, I., 2017. Las bioenergías en España. Una serie de producción, consumo y stocks entre 1860 y 2010. (No. 1702). Documentos de Trabajo de la Sociedad Española de Historia Agraria. Sociedad Española de Historia Agraria. (Available at https://ideas.repec.org/p/seh/wpaper/1702.html, accessed 22 March 2022).
Lambs, L., Muller, E., 2002. Sap flow and water transfer in the Garonne River riparian woodland, France: first results on poplar and willow. Ann. For. Sci. 59 (3), 301–315.
Lambs, L., Loubiat, M., Girel, J., Tissier, J., Peltier, J.-P., Marigo, G., 2006. Survival and acclimatation of *Populus nigra* to drier conditions after damming of an alpine river, southeast France. Ann. For. Sci. 63, 377–385.
Larsson, L.A., Larsson, P.O. 2018. CDendro and CooRecorder (v. 9.3.1) [software]. Cybis Elektronik and Data AB, Saltsjöbaden, Sweden. Available from http://www.cybis.se.
Lorimer, C.G., Frelich, L.E., 1989. A methodology for estimating canopy disturbance frequency and intensity in dense temperate forests. Can. J. For. Res. 19 (5), 651–663.
Luyssaert, S., Schulze, E.-D., Börner, A., Knohl, A., Hessenmöller, D., Law, B.E., Ciais, P., Grace, J., 2008. Old-growth forests as global carbon sinks. Nature 455 (7210), 213–215.
Moe, B., Botnen, A., 2000. Epiphytic vegetation on pollarded trunks of *Fraxinus excelsior* in four different habitats at Grinde, Leikanger, western Norway. Plant Ecol. 151, 143–159.
Norton, D.A., Palmer, J.G., Ogden, J., 1987. Dendroecological studies in New Zealand. 1. An evaluation of age estimates based on increment cores. New Zeal. J. Bot. 25, 373–383.
Nowacki, G.J., Abrams, M.D., 1997. Radial-growth averaging criteria for reconstructing disturbance histories from presettlement-origin oaks. Ecol. Monogr. 67 (2), 225–249.
Peterken, G., 1996. Natural woodland: ecology and conservation in northern temperate regions. Cambridge Univ. Press, Cambridge.
R Development Core Team. 2021. R: A Language and Environment for Statistical Computing. Vienna, Austria.
Rackam, G., 2006. Woodlands. Collins, London.
Ranius, T., Jansson, N., 2000. The influence of forest regrowth, original canopy cover and tree size on saproxylic beetles associated with old oaks. Biol. Conserv. 95 (1), 85–94.
Read, H.J., 1996. Pollard and Veteran Tree Management, Part II. Corporation of London, Burnham Beeches.
Read, H., 2000. Veteran Trees: A Guide to Good Management. English Nature. The Countryside Agency and English Heritage, Peterborough.
Read, H.J., 2003. A study of practical pollarding techniques in northern Europe. Report. (Available at https://www.ancienttreeforum.co.uk/wp-content/uploads/2017/05/A-study-of-practical-pollarding-techniques-in-northern.pdf, accessed 18 March 2022).
Read, H.J., 2008. Pollards and pollarding in Europe. British Wildlife 250–259.
Rohde, M.M., Stella, J.C., Roberts, D.A., Singer, M.B., 2021. Groundwater dependence of riparian woodlands and the disrupting effect of anthropogenically altered streamflow. Proc. Nat. Acad. Sci. USA 118, e2026453118.
Rood, S.B., Patiño, S., Coombs, K., Tyree, M.T., 2000. Branch sacrifice: cavitation-associated drought adaptation of riparian cottonwoods. Trees Struct. Funct. 14, 248–257.
Rood, S.B., Goater, L.A., Mahoney, J.M., Pearce, C.M., Smith, D.G., 2007. Floods, fire, and ice: disturbance ecology of riparian cottonwoods. Can. J. Bot. 85, 1019–1032.
Rozas, V., 2003. Tree age estimates in *Fagus sylvatica* and *Quercus robur*: testing previous and improved methods. Plant Ecol. 167, 193–212.
Rozas, V., 2004. A dendroecological reconstruction of age structure and past management in an old-growth pollarded parkland in northern Spain. For. Ecol. Manage. 195 (1-2), 205–219.
Sánchez-Pérez, J.M., Lucot, E., Bariac, T., Trémolières, M., 2008. Water uptake by trees in a riparian hardwood forest (Rhine floodplain, France). Hydrol. Proc. 22 (3), 366–375.
Scott, M.L., Shafroth, P.B., Auble, G.T., 1999. Responses of riparian cottonwoods to alluvial water table declines. Env. Manage. 23 (3), 347–358.
Šenfeldr, M., Horák, P., Kvasnica, J., Šrámek, M., Hornová, H., Maděra, P., 2021. Species-specific effects of groundwater level alteration on climate sensitivity of floodplain trees. Forests 12, 1178.
Singer, M.B., Stella, J.C., Dufour, S., Piégay, H., Wilson, R.J.S., Johnstone, L., 2013. Contrasting water-uptake and growth responses to drought in co-occurring riparian tree species. Ecohydrology 6 (3), 402–412.
Singer, M.B., Sargeant, C.I., Piégay, H., Riquier, J., Wilson, R.J.S., Evans, C.M., 2014. Floodplain ecohydrology: Climatic, anthropogenic, and local physical controls on partitioning of water sources to riparian trees. Water Res. Res. 50 (5), 4490–4513.
Stella, J. C., Bendix, J., 2019. Multiple stressors in riparian ecosystems. In: Multiple Stressors in River Ecosystems, Sabater, S., Elosegi, A., Ludwig R., (eds.), Elsevier, Amsterdam, pp. 81–110.
Turok, J., Lefèvre, F., de Vries, S., Tóth, B., (compilers) 1997. Populus nigra Network. Report of the third meeting, 5-7 October 1996, Sárvár, Hungary. International Plant Genetic Resources Institute, Rome, Italy.
Solans, M.A., Poff, N.L., 2013. Classification of natural flow regimes in the Ebro basin (Spain) by using a wide range of hydrologic parameters. River Res. Appl. 29 (9), 1147–1163.
Vicente-Serrano, S.M., Beguería, S., López-Moreno, J.I., 2010. A multiscalar drought index sensitive to global warming: the standardized precipitation evapotranspiration index. J. Clim. 23, 1696–1718.
Wigley, T.M.L., Briffa, K.R., Jones, P.D., 1984. On the average value of correlated time series, with applications in dendroclimatology and hydrometeorology. J. Clim. Appl. Meteorol. 23 (2), 201–213.